www.sciencemag.org/cgi/content/full/science.1188070/DC1

Supporting Online Material for

Endosomal Chloride-Proton Exchange Rather Than Chloride Conductance is Crucial for Renal Endocytosis

Gaia Novarino, Stefanie Weinert, Gesa Rickheit, Thomas J. Jentsch*

*To whom correspondence should be addressed. E-mail: jentsch@fmp-berlin.de

Published 29 April 2010 on *Science* Express
DOI: 10.1126/science.1188070

This PDF file includes:

Supporting Online Material for

Endosomal Chloride-Proton Exchange Rather Than Chloride Conductance is Crucial for Renal Endocytosis

Gaia Novarino, Stefanie Weinert, Gesa Rickheit & Thomas J. Jentsch

* To whom correspondence should be addressed E-mail: jentsch@fmp-berlin.de

This PDF file includes:

Materials and Methods

Mice

The generation of *Clcn5* ⁻ mice has been described previously (*1*). For the generation of knock-in mice genomic *Clcn5* DNA isolated from a mouse λFixII 129/Sv library (Stratagene) was cloned into a pKO 901 Scrambler vector (Lexicon Genetics Incorporated) and used to create the targeting constructs shown in Fig. S1A and S4A. Pgk promoter-driven diphtheria toxin A fragment (dtA) was used to select against random integration. Additionally, a neomycin selection cassette flanked by FRT sites (*Clcn5* *) or loxP sites (*Clcn5* ^{unc}) was inserted. The linearized vectors were electroporated into E14 (*Clcn5* ^{unc}) or R1 (*Clcn5* *) embryonic stem cells. DNA from neomycin-resistant clones was digested using *Acc*65I and analyzed by Southern blot using an external 400 bp (*Clcn5* ^{unc}) or 600 bp (*Clcn5* *) probe. Cells from a correctly targeted clone were injected into C57Bl/6J blastocysts that were implanted into foster mothers. To remove the neomycin cassette chimeric males were bred with cre-recombinase expressing 'deleter' mice (*2*), resulting in the **unc**oupled *Clcn5* ^{unc} allele, or with FLPeR mice (*3*) resulting in the *Clcn5* * allele. *Clcn5* ^{unc} and *Clcn5* * mice were born at approximately Mendelian ratio and survived normally. Experiments were performed with mice in a mixed C57Bl/6-129/Svj genetic background, always using littermates as controls.

Sequencing

Targeting constructs were completely sequenced on ABI 3730 DNA analyzer (Applied Biosystems). The entire open reading frame of *Clcn5* ^{unc} was amplified by RT-PCR in 5 pieces from mRNA extracted from kidneys of *Clcn5* $^{unc/y}$ mice and sequenced to verify the presence of the E211A mutation and the absence of fortuitous other mutations.

RNA expression analysis

Total kidney RNA was extracted from adult *Clcn5* ^{unc} and wild-type littermates using Trizol (Invitrogen) reagent and the High-Pure RNA purification kit (QIAGEN). RNA was transcribed into cDNA using the SuperScript II cDNA kit (Invitrogen) with random hexamers. Real-time PCR was performed using the 7900 HT cycler from Applied Biosystems and the SYBR Green Power PCR master mix (Applied Biosystems) and normalized to HPRT (hypoxanthine phosphoribosyltransferase). An initial denaturation step (10 min at 95℃) was followed by 40 cycles with two steps: 95℃ for 15 s, followed by 60℃ for 60 s. Each sample was amplified in duplicate and gave consistent results in two independent experiments. The value of the wild-type animals was set to 100. RNA values from *Clcn5* ^{unc} animals are shown as *%* of the wild-type. Contamination with genomic DNA was negligible.

Western blot

30 µg of kidney membrane preparation (140,000 x g pellet) were separated by SDS-PAGE using 8.5% acrylamide gels. For megalin analysis we used 3-8% NuPAGE Tris-acetate gels with NuPAGE Tris-Acetate SDS Running Buffer (Invitrogen).

In vivo endocytosis experiments
Bovine β-lactoglobulin (Sigma Aldrich) labeled with Alexa Fluor 546 (Invitrogen) or Alexa Fluor 488-dextran (10 kDa; Invitrogen) was injected into the vena cava of anesthetized mice. After 7 minutes kidneys were perfused with PBS for 3 minutes and subsequently with 4% PFA.

Immunohistochemistry and antibodies
Mice were fixed by perfusion with 4% (w/v) PFA, tissues dissected and sucrose embedded for cryosectioning. The following primary antibodies were used: rabbit PEP5A (N-terminus, ClC-5NT) and PEP5E (C-terminus, ClC-5CT) against ClC-5 (*4*), rabbit anti-ClC-3 (ab#1035) and rabbit anti-ClC-4 (ab#1261) as described (*5*), guinea pig anti-AE1 (*6*), mouse anti-villin (Acris), guinea pig anti-megalin (*7*), rabbit anti-cubilin (*8*), rabbit anti-β-actin (Sigma Aldrich). The antibody against NaPi-2a was generated in rabbits against the two peptides CYARPEPRSPQLPPRV and CPSPRLALPAHHNATRL, and the rabbit C5/05A antibody against the peptide CQDPDSILFN representing the C-terminus of ClC-5 (ClC-5CT). Peptides were coupled to keyhole limpet hemocyanin (KLH) via the C-terminalcysteine residues. Guinea pig ClC-5 antibody was raised against the same amino-terminal peptide as PEP-5A (*1*). Specificity of affinity-purified antibodies was checked using *Clcn5*$^{-}$ mice. Secondary antibodies conjugated to Alexa Fluor 488, 546 or 633 (Invitrogen) or HRP (Jackson ImmunoResearch) were used.

Image acquisition
All images were acquired using a confocal microscope (LSM510, Zeiss).

Serum and urine analysis
Blood was drawn from the retro-orbital sinus under light ether anesthesia. Mice were kept in metabolic cages for urine collection. Blood and urine proteins, glucose and salts were determined by Dr. D. Becker (Institut für Labormedizin, Helios Klinikum Berlin-Buch). Urine pH was measured with a standard glass electrode. Serum 25(OH)-D3 and 1,25$(OH)_2$-D3 were determined using ELISA assays (Immunodiagnostic Systems GmbH). Urine samples were normalized to creatinine values and analyzed by SDS–PAGE followed by silver staining or Western blotting using polyclonal antibodies against retinol binding protein (from W.S. Blaner, Cleveland) or vitamin D binding protein (Dako).

Acidification assay
For ATP-driven acidification assay endosome-enriched vesicles were prepared as described previously (*9*). Briefly, vesicles were prepared from kidneys from 2-4 mice of the same genotype and pooled. Animals were killed, kidneys were taken out and the renal cortex (consisting of ~80% proximal tubules) was dissected in ice cold PBS. All the subsequent steps were performed at 4 ℃. When pooling kidneys from 4 animals, the tissue was homogenized in 30 ml of homogenization buffer (300 mM mannitol, 12 mM HEPES/Tris pH 7.4) with 20 strokes in a loose-fitting glass/Teflon Potter homogenizer (1,200 rpm) (B. Braun). After homogenization, the suspension was centrifuged at 2,500 x g for 15 min. The pellet was discarded and the supernatant was centrifuged at 20,000 x g for 20 min. Most of the resulting

supernatant (S) was decanted and saved. The rest of the supernatant (about 1 ml) was used to disperse the fluffy upper part of the pellet by careful swirling of the tube. Supernatant S and the dispersed fluffy pellet were combined and centrifuged at 48,000 x g for 30 min. After centrifugation supernatant was discarded. Pellets containing crude plasma membranes and endocytic vesicles were resuspended and centrifuged at 48,000 x g for 30 min in a 16% Percoll gradient to separate endocytic vesicles from other membranes. After centrifugation the lowest 3 ml were taken and 27 ml of a potassium buffer (300 mM mannitol, 100 mM K^+ gluconate, 5 mM $MgSO_4$, 5 mM HEPES/Tris pH 7.0) were added. This vesicle suspension was incubated for 30 minutes on ice and subsequently centrifuged at 48,000 x g for 30 min. Supernatant was discarded. The pellet was resuspended in 1 ml potassium buffer and centrifuged at 2,500 x g for 15 min. The pellet, which contains endocytic vesicles, was resuspended in 50 µl of potassium buffer. The vesicle suspension was kept at 0-4° C at a concentration of 4 mg/ml for a maximum of 2 hours before performing the acidification assay. A vesicle suspension aliquot containing 200 µg protein (as determined by BCA assay) was suspended in a chloride buffer (maintained at 37 ^oC) containing: 300 mM mannitol, 100 mM KCl, 5 mM $MgSO_4$, 6 µM acridine orange, 5 mM HEPES/Tris, pH 7.0. The pH-sensitive fluorescence of acridine orange was monitored during continuous stirring with a Xenius spectrofluorometer (Safas) (excitation 492 nm, emission 530 nm). Once fluorescence baseline was stable, the assay was started. Na-ATP (final concentration 1.5 mM) and FCCP (final concentration 10 µM) were injected in the cuvette using an automatic injector system. The immediate increase in acridine orange fluorescence observed after addition of ATP is an artifact due to the interaction of the dye and ATP (*10*). For evaluation and comparing acidification (Fig. 1C, D), we included only measurements in which the peak upon ATP addition was between 1.0 and 1.3 fluorescence ratios, indicating that speed of mixing and other parameters were in a similar range. Most of the acidification assay experiments were performed by experimenters blinded to the genotype.

Electrophysiological analysis of ClC-5 mutants expressed in *Xenopus* oocytes

Pieces of ovary were obtained by surgery from deeply anesthetized (0.1% tricaine; Sigma-Aldrich) *Xenopus laevis* frogs. Oocytes were prepared by manual dissection and collagenase A (Roche Applied Science) digestion. 5 ng of wild-type or negative-tagged ClC-5 cRNA were injected into oocytes which were kept in ND96 solution (containing 96 mM NaCl, 2 mM KCl, 1.8 mM $CaCl_2$, 1 mM $MgCl_2$, 5 mM HEPES, pH 7.5) at 17 ℃ for 2 days. Two-electrode voltage-clamping was performed at room temperature (20–24 ℃) using a TEC10 amplifier (npi Electronics) and pClamp9 software (Molecular Devices). The standard bath solution contained 96 mM NaCl, 2 mM K^+ gluconate, 5 mM Ca^{2+} D-gluconate, 1.2 mM $MgSO_4$, 5 mM HEPES, pH 7.5.

Data analysis and statistical methods

For figure 1 data were analyzed using software SAFAS SP2000 (SAFAS) and Origin 7.5 (OriginLab Corporation). Significance was determined using a two-tailed Student's t-test

Supporting figures and legends

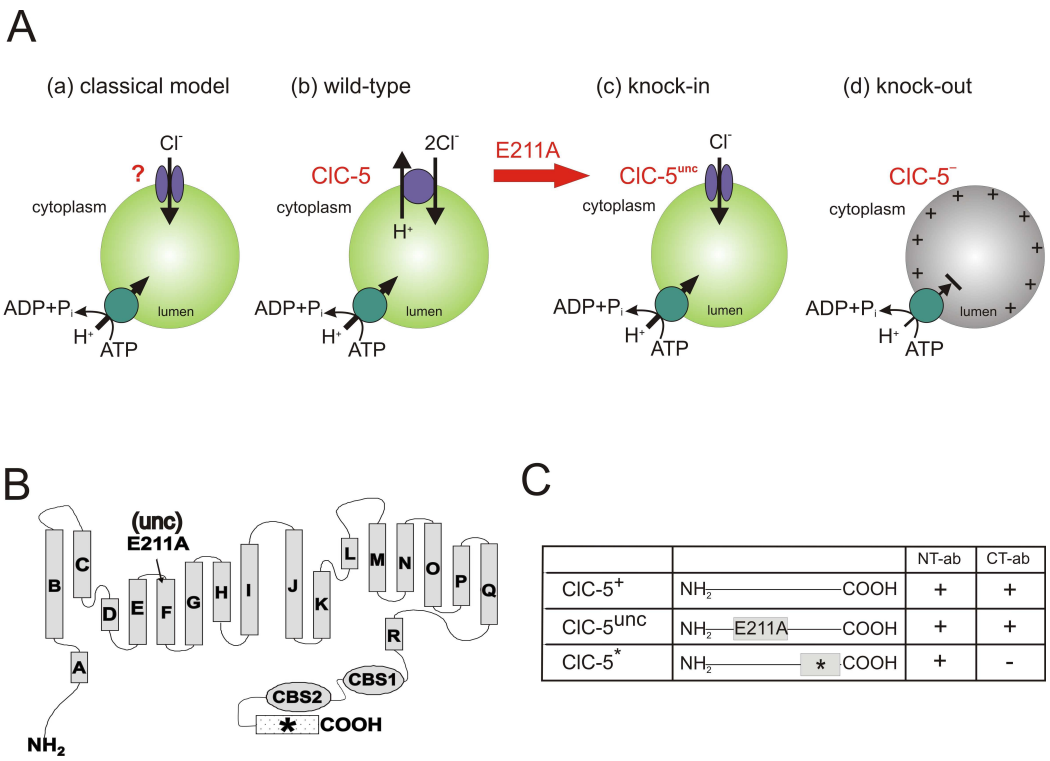

C

		NT-ab	CT-ab
ClC-5+	NH_2——COOH	+	+
ClC-5unc	NH_2—E211A—COOH	+	+
ClC-5*	NH_2——*COOH	+	-

Fig. S1. **Knock-in mice converting ClC-5 into a chloride conductor.** (**A**) Models for endosomal acidification. In the classical model (a) a Cl^- channel supplies countercurrent for the proton pump, but in reality a Cl^-/H^+-exchanger performs this role (b). An uncoupling point mutation converts ClC-5 into a pure conductor (c), going back to 'classics' (a). In the knock-out (d) luminal charge accumulation blocks acidification. (**B**) CLC topology model indicating positions of the uncoupling E211A (unc) mutation and the negative tag (*****) in which the extreme C-terminus of ClC-5 is converted into that of ClC-3 (fig S5). (**C**) ClC-5 variants expressed in WT and knock-in mice and their recognition by our N-terminal and C-terminal antibodies.

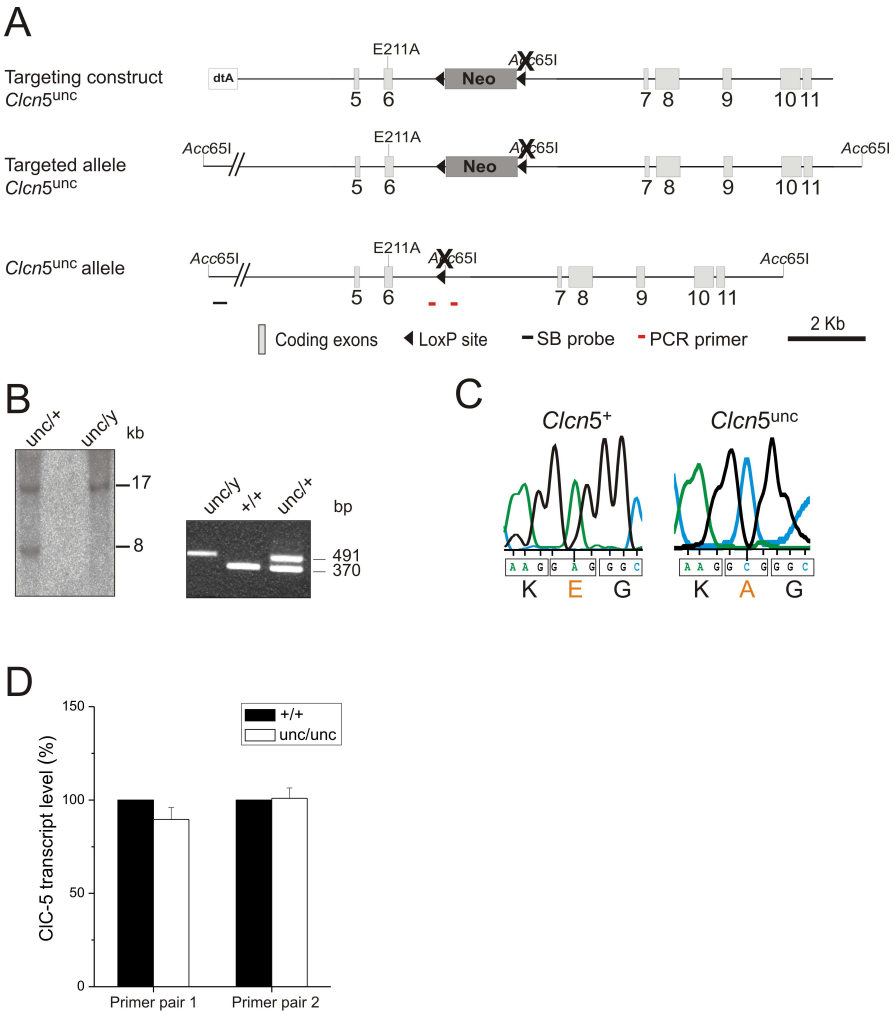

Fig. S2. Generation of knock-in mice carrying the uncoupling *Clcn5* ^{unc} allele. (**A**) Targeting strategy. The targeting construct (top) contained 13 kb of mouse genomic sequence that was modified by inserting the uncoupling E211A mutation into exon 6 and a neomycin selection cassette (flanked by loxP sites) between exons 6 and 7. The *Acc*65I restriction site that was used for neomycin cassette insertion was destroyed in the cloning process. A diphtheria toxin A (dtA) cassette was added at the 5' end to select against random integration. Removal of the neomycin cassette in vivo resulted in the ***unc***oupled *Clcn5* ^{unc} allele (bottom). (**B**) Southern blot analysis of *Acc*65I-digested genomic DNA (left) and genotyping PCR (right) using the hybridization probe and PCR primers, respectively, indicated in (A). The sequences of PCR primers were: 5´-ATGTGTGCAGCAGATGTGTGCC-3´, 5´-CAACCTTCAGCACCACAAAAGC-3´. (**C**) DNA sequence obtained from RT-PCR-amplified kidney mRNA confirms the presence of the E211A mutation. (**D**) Quantitative real-time PCR on mRNA extracted from WT and *Clcn5* $^{unc/unc}$ kidneys shows similar mRNA levels for the WT and *Clcn5* ^{unc} allele. RNA levels are shown as % ± SD of WT values that were set to 100 (2 animals per genotype). Primer pairs used: 5´-CTTCATGTACGTCCTCTGGGCT-CTTCTGTT-3´ and 5´-CCAGGGGGCCCGCCTTGCCCAGGCTCAAGCC-3´; 5´-GCCTGGGCAAGGCGGGCCCCCTGGTGCACGTGGC and 5´-GGAAGA-GGTCAGCTACTAC-3´.

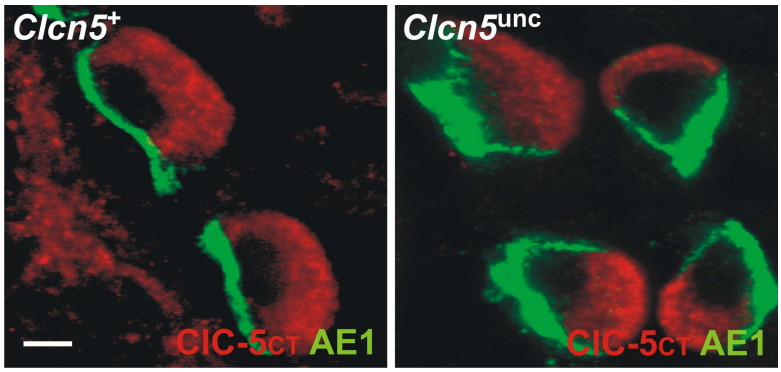

Fig. S3. Localization of ClC-5 in intercalated cells. Identical staining pattern using the C-terminal PEP5E ClC-5 antibody (*4*) in distal tubular intercalated cells of WT and *Clcn5* $^{unc/y}$ mice. Intercalated cells show basolateral staining (green) for the anion exchanger AE1. Scale bar 2.7 µm.

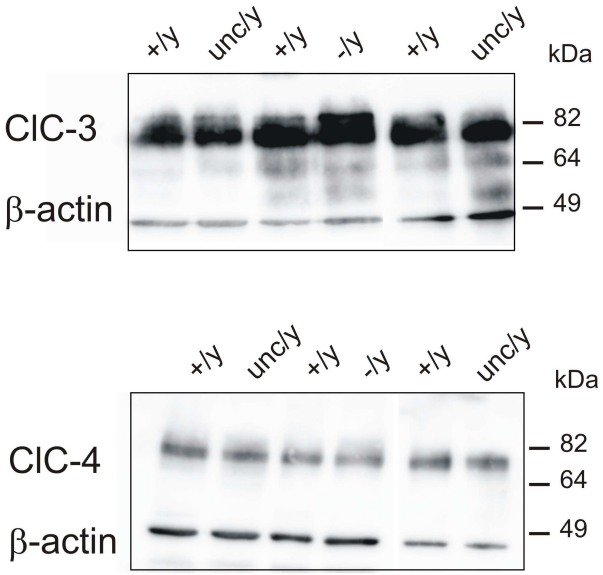

Fig. S4. Expression of ClC-3 and ClC-4 in kidneys of *Clcn5* $^{+}$, *Clcn5* $^{-}$ and *Clcn5* ^{unc} mice. Membrane proteins from kidneys of the indicated genotypes were separated by SDS-PAGE and analyzed in Western blot experiments with antibodies against ClC-3 and ClC-4 (ab#1035 and #1261 described by Maritzen *et al.* (*5*)). There is no upregulation of these close homologues of ClC-5 neither in *Clcn5* $^{-}$ nor in *Clcn5* ^{unc} kidneys.

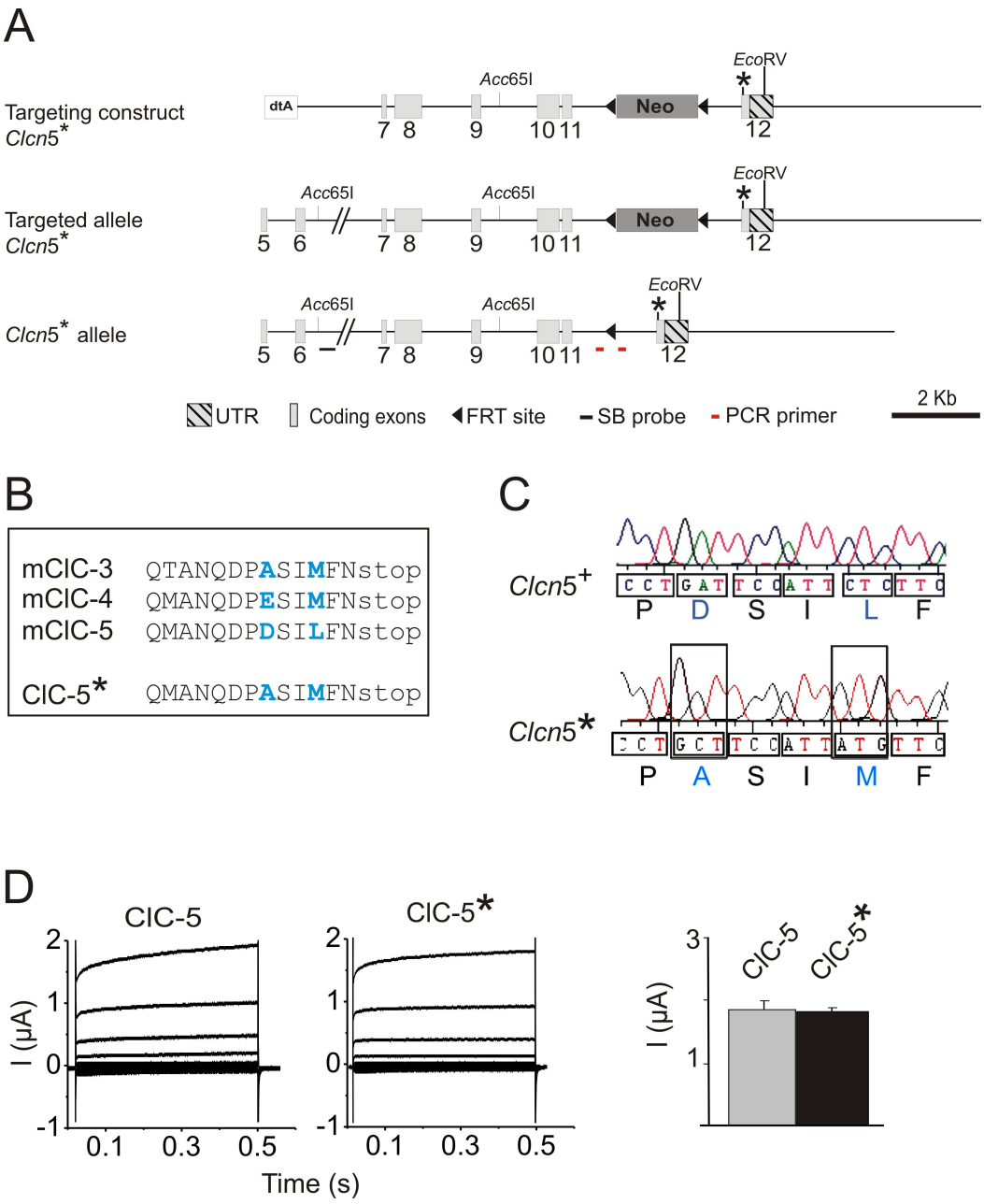

Fig. S5. Generation of knock-in mice carrying the 'negatively tagged' *Clcn5* * allele. (**A**) Targeting strategy. Top, targeting construct containing 12.5 kb of mouse genomic DNA, which has been modified by changing four base pairs in exon 12 that mutate two amino-acids of the extreme carboxyterminus (indicated by an asterisk "*"). An *Acc*65I site was inserted between exons 9 and 10 for screening purposes. Additionally, a neomycin selection cassette flanked by FRT sites has been inserted into the intron preceding exon 12, and a diphtheria toxin A (dtA) cassette has been added to the 5' end to select against non-homologous recombination. In vivo excision of the selection cassette resulted in the *Clcn5* * allele (bottom). PCR primers used for genotyping were 5´-GCTCTCGTAAAGCATTTACTATGC-3´ and 5´-GTAT-AGGCTGAGGAGAGTGTT-3´. (**B**) Sequence comparison of the extreme C-

terminus of mouse ClC-3, -4, and -5 proteins that form a distinct branch of the CLC gene family. Non-conserved amino-acids are shown in blue. Since two antibodies generated against C-terminal peptides of ClC-5 (the PEP5E antibody (*4*) and the newly generated C5/05A antibody) recognize ClC-5, while showing almost no cross-reactivity against ClC-3, we created a 'negatively tagged' ClC-5 (ClC-5*) by minimally changing its C-terminal sequence by converting it to that of ClC-3. This minimal alteration of ClC-5 did not affect its function. (**C**) Confirmation of changed C-terminus by sequencing genomic DNA from WT and *Clcn5* * mice. (**D**) Unchanged electrophysiological properties of the ClC-5* mutant transporter. *Xenopus* oocytes were injected with cRNA (5 ng) and examined by two-electrode voltage-clamping as described previously (*11*), using a protocol that clamped the voltage to values between -125 and + 100 mV. Typical original traces are shown at left, and mean currents at + 100 mV at right (n=10, ± SEM). These currents reflect electrogenic $2Cl^-/H^+$-exchange. Mean currents and original traces are modified from (*12*).

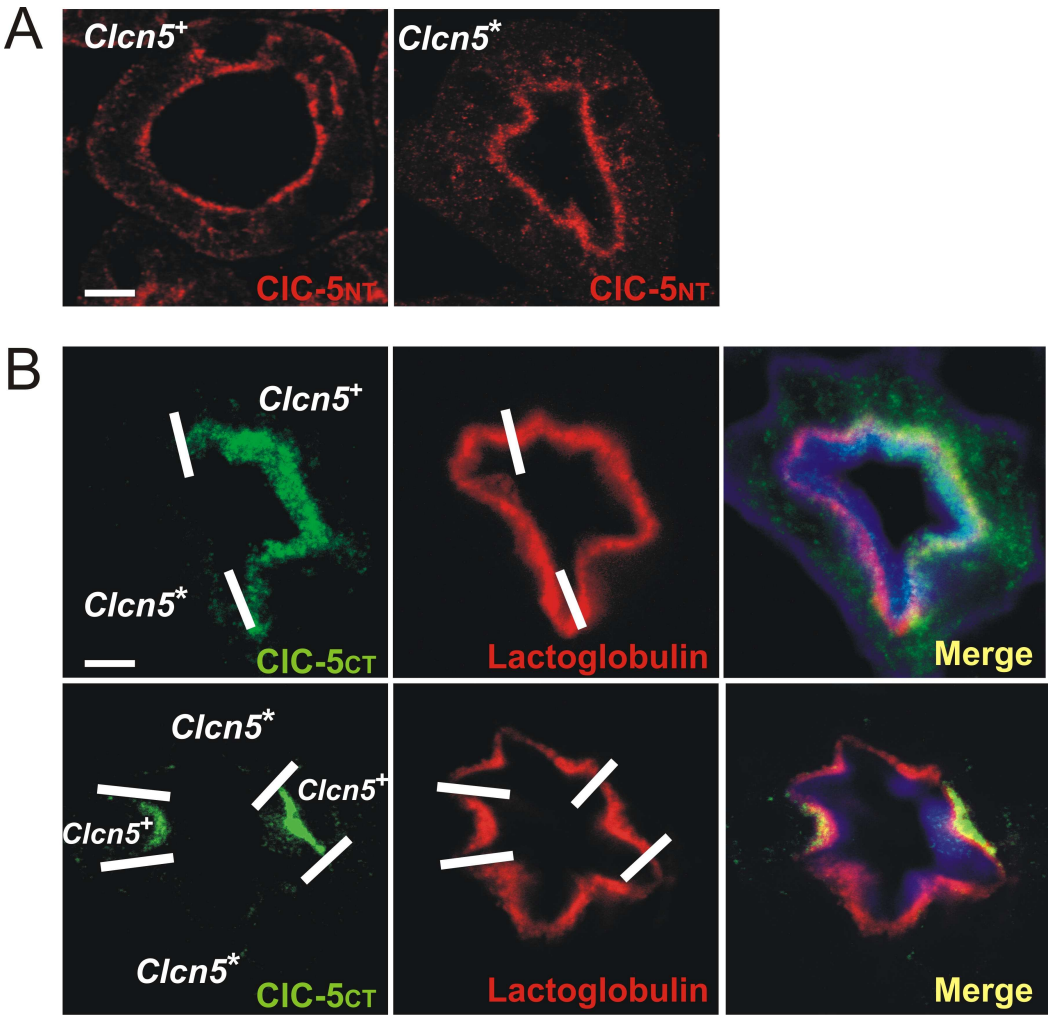

Fig. S6. Analysis of 'negatively tagged' *Clcn5* * cells. (**A**) Subcellular localization of WT (left) and the negatively tagged ClC-5* (right) protein in proximal tubular cells. No difference in localization was observed. (**B**) In vivo endocytosis of Alexa Fluor 546-labeled β-lactoglobulin in proximal tubules of female *Clcn5* $^{+/*}$ mice expressing side by side either WT ClC-5 (labeled *Clcn5* $^{+}$) or 'negatively tagged' ClC-5* (labeled *Clcn5* *). Only ClC-5^{+} is recognized by the C-terminal ClC-5 antibody C5/05A, resulting in green staining (left panels). *Clcn5* *- and *Clcn5* $^{+}$-expressing cells show indistinguishable accumulation of β-lactoglobulin (stained in red, center panels) which was stopped after a 10 min uptake period. Right panels show overlay, with additional staining for the brush border protein villin in blue. Scale bar, 6 µm for (A) and 5 µm for (B).

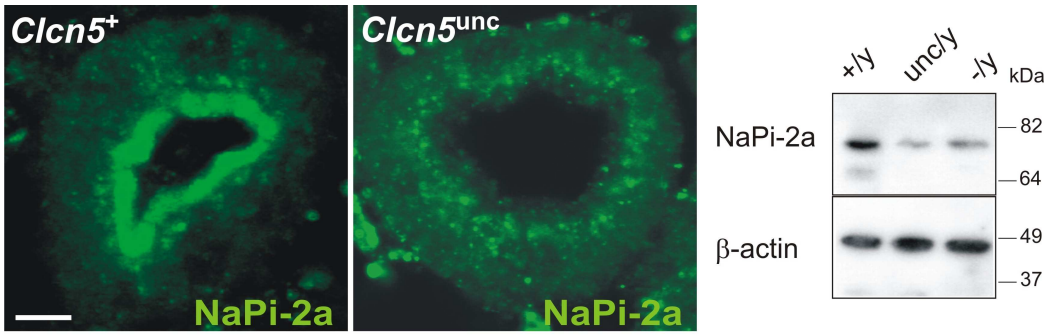

Fig. S7. NaPi-2a expression in proximal tubule cells. Reduced expression and intracellular localization of NaPi-2a in proximal tubular cells expressing ClC-5^{unc} instead of WT ClC-5. Right, similar reduction of NaPi-2a in Western blot of *Clcn5* $^{-/y}$ and *ClC-5*$^{unc/y}$ kidney membranes. Scale bar, 5 µm.

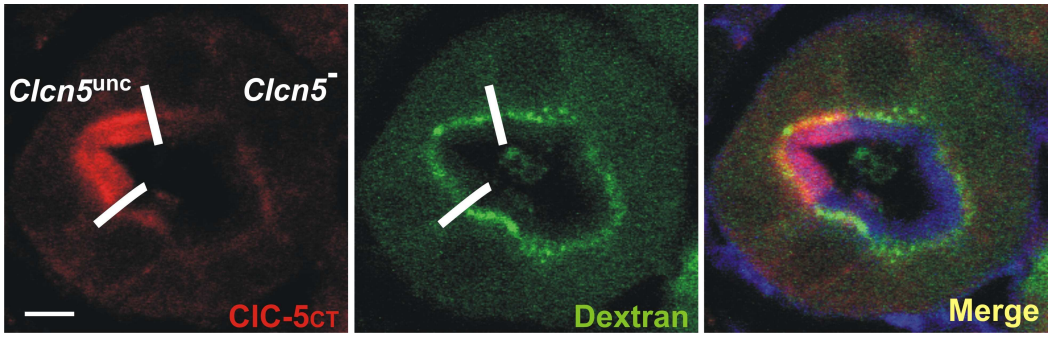

Fig. S8. Fluid-phase endocytosis in *Clcn5* ^{unc} and *Clcn5* $^{-}$ proximal tubule cells. No difference in uptake of labeled dextran between cells lacking ClC-5 (*Clcn5* $^{-}$) or expressing *Clcn5* ^{unc} in a chimeric tubule from a *Clcn5* $^{unc/-}$ female. Scale bar, 5 µm.

Table S1

Serum and urinary parameters

A

	Clcn5 $^{+/y}$	*Clcn5* $^{unc/y}$
serum concentrations (mmol/l)		
Ca	2.56 ± 0.13 (10)	2.64 ± 0.16 (10)
Pi	2.33 ± 0.38 (10)	2.77 ± 0.64 (10)
Na	153.07 ± 5.31 (10)	157.48 ± 6.13 (10)
Cl	115.84 ± 4.73 (10)	111.12 ± 5.38 (10)
K	5.28 ± 0.50 (10)	5.42 ± 0.26 (10)
glucose	7.88 ±1.04 (10)	5.96 ±1.49 (10)
creatinine (µmol/l)	14.75 ± 4.06 (10)	15.57 ± 6.97 (10)
insulin (pg/ml)	2490 ± 935 (10)	2261 ± 1103 (10)

B

	Clcn5 $^{+/y}$	*Clcn5* $^{unc/y}$	*Clcn5* $^{+/y}$	*Clcn5* $^{-/y}$
urine concentrations (mmol/mmol creatinine)				
Ca/creatinine	1.77 ± 0.15 (40)	3.19 ± 0.20 ***(40)	1.88 ± 0.12 (20)	2.39 ± 0.21 (20)
Pi/creatinine	6.04± 0.87 (40)	11.49± 0.88 ***(40)	5.01 ± 0.79 (20)	7.98 ± 1.13* (20)
Na/creatinine	56.90 ± 2.63 (20)	59.39 ± 2.44 (20)	55.86 ± 1.57 (20)	53.18 ± 1.78 (20)
Cl/creatinine	112.84 ± 7.53 (20)	93.52 ± 8.30 (20)	128.08 ± 4.06 (20)	106.88 ± 2.67 (20)
K/creatinine	108.33 ± 4.30 (20)	129.07 ± 5.63 *(20)	125.95 ± 2.76 (20)	110.42 ± 3.44 * (20)
Mg/creatinine	6.46 ± 0.69 (20)	9.28 ± 0.87 (20)	8.84 ± 0.41 (20)	8.44 ± 0.74 (20)
glucose/creatinine	1.30± 0.21 (40)	4.53 ± 0.82 ***(40)	1.36 ± 0.16 (20)	2.74 ±0.44 * (20)
creatinine (mmol/l)	2.65 ± 0.27 (40)	1.05 ± 0.27 **(40)	2.23 ± 0.29 (20)	2.11 ± 0.56 (20)
insulin (pg/ml)	161.6 ± 147 (20)	5160 ± 1761* (20)	223 ± 79 (20)	5166 ± 288* (20)
pH	7.27 ± 0.28 (20)	6.25 ± 0.33 * (20)	7.20 ± 0.09 (20)	6.81 ± 0.07 * (20)
urinary volume (ml/day)	1.92 ± 0.20 (40)	4.90 ± 0.46 ***(40)	1.92 ± 0.12 (20)	2.36 ± 0.41 (20)

*** p< 0.0005 , ** p<0,001, * p<0,01 The number of determinations is indicated in brackets. Data are mean values ± SEM. *Clcn5*$^{+/y}$columns represent control littermates of the genetically modified mice in the respective columns at the right.

Supporting References

1. N. Piwon, W. Günther, M. Schwake, M. R. Bösl, T. J. Jentsch, ClC-5 Cl^--channel disruption impairs endocytosis in a mouse model for Dent's disease. *Nature* 408, 369 (2000).
2. F. Schwenk, U. Baron, K. Rajewsky, A cre-transgenic mouse strain for the ubiquitous deletion of *loxP*-flanked gene segments including deletion in germ cells. *Nucleic Acids Res* 23, 5080 (1995).
3. F. W. Farley, P. Soriano, L. S. Steffen, S. M. Dymecki, Widespread recombinase expression using FLPeR (flipper) mice. *Genesis* 28, 106 (2000).
4. W. Günther, A. Lüchow, F. Cluzeaud, A. Vandewalle, T. J. Jentsch, ClC-5, the chloride channel mutated in Dent's disease, colocalizes with the proton pump in endocytotically active kidney cells. *Proc Natl Acad Sci U S A* 95, 8075 (1998).
5. T. Maritzen, D. J. Keating, I. Neagoe, A. A. Zdebik, T. J. Jentsch, Role of the vesicular chloride transporter ClC-3 in neuroendocrine tissue. *J Neurosci* 28, 10587 (2008).
6. N. Schulz, M. H. Dave, P. A. Stehberger, T. Chau, C. A. Wagner, Differential localization of vacuolar H^+-ATPases containing a1, a2, a3, or a4 (ATP6V0A1-4) subunit isoforms along the nephron. *Cell Physiol Biochem* 20, 109 (2007).
7. C. Kastner *et al.*, Effects of receptor-mediated endocytosis and tubular protein composition on volume retention in experimental glomerulonephritis. *Am J Physiol Renal Physiol* 296, F902 (2009).
8. P. J. Verroust, Pathophysiology of cubilin: of rats, dogs and men. *Nephrol Dial Transplant* 17 Suppl 9, 55 (2002).
9. I. Sabolić, G. Burckhardt, Characteristics of the proton pump in rat renal cortical endocytotic vesicles. *Am J Physiol* 250, F817 (1986).
10. Y. Moriyama, T. Takano, S. Ohkuma, Acridine orange as a fluorescent probe for lysosomal proton pump. *J Biochem* 92, 1333 (1982).
11. T. Friedrich, T. Breiderhoff, T. J. Jentsch, Mutational analysis demonstrates that ClC-4 and ClC-5 directly mediate plasma membrane currents. *J Biol Chem* 274, 896 (1999).
12. G. Rickheit *et al.*, Role of ClC-5 in renal endocytosis is unique among CLC exchangers and does not require PY-motif-dependent ubiquitylation. *J Biol Chem*, electronic prepub (2010).